A new type III effector from Bradyrhizobium sp. DOA9 encoding a putative SUMO-protease blocks nodulation in Arachis hypogaea L.

Beedou Aphaiso, Pongdet Piromyou, Pakpoom Boonchuen, Pongpan Songwattana, Jenjira Wongdee, Teerana Greetatorn, Kamonluck Teamtisong, Alicia Camuel, Panlada Tittabutr, Nantakorn Boonkerd, et al.

▶ **To cite this version:**

Beedou Aphaiso, Pongdet Piromyou, Pakpoom Boonchuen, Pongpan Songwattana, Jenjira Wongdee, et al.. A new type III effector from Bradyrhizobium sp. DOA9 encoding a putative SUMO-protease blocks nodulation in Arachis hypogaea L.. Scientific Reports, 2024, 14, pp.31646. 10.1038/s41598-024-78913-2 . hal-04906316

HAL Id: hal-04906316
https://hal.inrae.fr/hal-04906316v1

Submitted on 22 Jan 2025

HAL is a multi-disciplinary open access archive for the deposit and dissemination of scientific research documents, whether they are published or not. The documents may come from teaching and research institutions in France or abroad, or from public or private research centers.

L'archive ouverte pluridisciplinaire **HAL**, est destinée au dépôt et à la diffusion de documents scientifiques de niveau recherche, publiés ou non, émanant des établissements d'enseignement et de recherche français ou étrangers, des laboratoires publics ou privés.

Distributed under a Creative Commons Attribution - NonCommercial - NoDerivatives 4.0 International License

scientific reports

Check for updates

OPEN

A new type III effector from *Bradyrhizobium* sp. DOA9 encoding a putative SUMO-protease blocks nodulation in *Arachis hypogaea* L.

Beedou Aphaiso[1,5], Pongdet Piromyou[2], Pakpoom Boonchuen[1], Pongpan Songwattana[2], Jenjira Wongdee[2], Teerana Greetatorn[2], Kamonluck Teamtisong[3], Alicia Camuel[4], Panlada Tittabutr[1], Nantakorn Boonkerd[1], Eric Giraud[4]✉ & Neung Teaumroong[1]✉

Effector proteins secreted via the type III secretion system (T3SS) of nitrogen-fixing rhizobia are key determinants of symbiotic compatibility in legumes. Previous report revealed that the T3SS of *Bradyrhizobium* sp. DOA9 plays negative effects on *Arachis hypogaea* symbiosis. In this study, we characterized the symbiotic role of 4 effector proteins (p0490, p0871, SkP48, and p0903) containing the small ubiquitin-like modifier (SUMO) protease domain identified in DOA9 during symbiosis. While the DOA9 strain and the two mutants of SUMO-proteases, p0490 and p0871, induced inefficient nodulation in *A. hypogaea*, the mutation of SUMO-proteases SkP48 or p0903 promoted efficient symbiosis comparable to the type strain *Bradyrhizobium arachidis* CCBAU051107. Complementation study of Δ*p0903* with various mutated forms of p0903 highlighted importance of ubiquitin-like protein (ULP) domain in restriction of nodulation in *A. hypogaea*. We observed the accumulation of jasmonic acid (JA) and upregulation of several defence genes involved in the JA/ethylene (ET) signalling pathway at the early stage of infection in roots inoculated with DOA9 strain compared with those inoculated with the DOA9-Δ*p0903* strain. Our data highlight the importance of SUMO-protease effectors during the symbiotic interaction between bradyrhizobia and *A. hypogaea*, which could be useful for the development of high-performance inocula to improve its growth.

Keywords *Bradyrhizobium* sp, *Arachis hypogaea*, T3SS, and SUMO-protease

The symbiotic relationship between rhizobia and legumes represents a fascinating and complex biological process with significant agronomical and ecological importance. This interaction begins when nitrogen-fixing rhizobia release signalling molecules called Nod factors (NFs), which trigger the formation of root nodules and facilitate bacterial infection. Within these nodules, rhizobia convert atmospheric nitrogen into a plant-accessible form in exchange for photosynthates and other nutrients from the host plant. Among rhizobia, *Bradyrhizobium* strains are particularly valuable in agriculture because of their ability to form symbioses with economically important legume crops such as soybeans, peanuts, and cowpeas[1–3]. This mutually beneficial partnership has attracted considerable scientific interest, as it plays a crucial role in sustainable agriculture and global nitrogen cycling.

In several strains of *Bradyrhizobium*, a type III secretion system (T3SS) plays a crucial role during symbiosis, significantly influencing the interaction with host plants[4,5]. The T3SS serves as a nanosyringe structure found in Gram-negative bacteria. Its function is to deliver type III effectors (T3Es) into eukaryotic host cells during interaction with the host[6]. As observed in pathogenic bacteria, the T3Es identified in rhizobia, often referred to as nodulation outer proteins (Nops), can act as double-edged swords, depending on the host plant[7]. They can promote symbiosis by suppressing the plant's immune system; however, if recognized by plant resistance proteins, they can trigger an immune response known as effector-triggered immunity (ETI), which can block

[1]School of Biotechnology, Institute of Agricultural Technology, Suranaree University of Technology, Nakhon Ratchasima 30000, Thailand. [2]Institute of Research and Development, Suranaree University of Technology, Nakhon Ratchasima 30000, Thailand. [3]The Center for Scientific and Technological Equipment, Suranaree University of Technology, Nakhon Ratchasima 30000, Thailand. [4]IRD/CIRAD/INRAE, PHIM, Plant Health Institute of Montpellier, UMR-PHIM, Université de Montpellier/Institut Agro, Montpellier 34398, France. [5]Deparment of plant science, Faculty of Agriculture and environment, Savannakhet University, Savannakhet 14, Kaysone Phomvihane, Laos. ✉email: eric.giraud@ird.fr; neung@sut.ac.th

rhizobial infection. This dual functionality highlights the complex interplay between rhizobia and their host plants, whereby the same effector proteins can either facilitate or hinder symbiosis based on the plant's immune recognition mechanisms. Moreover, the diverse array of T3Es identified in rhizobial strains contributes to host genotype-specific compatibility or incompatibility across various legume species, highlighting the intricate nature of rhizobia–legume interactions[8,9].

Our knowledge concerning the impact of T3Es on the symbiotic interaction of rhizobia with *Arachis hypogaea* L. (peanut) remains extremely limited, despite this genus being the second most important legume crop after soybean. Moreover, peanut plays a crucial role in sustainable agriculture and food security worldwide, particularly in developing countries, because of its nutritional value and the importance of its symbiosis with rhizobia[10]. Compared with the case of no inoculation, *Bradyrhizobium* inoculation increased the pod yield by 40%, reducing the need for nitrogen chemical fertilizers[11]. The symbiosis between peanuts and rhizobia not only reduces the need for chemical fertilizers but also contributes to improved soil health, making peanuts a uniquely sustainable crop in the face of growing agricultural challenges[12]. Thus, as the global demand for peanuts continues to rise, understanding and optimizing this symbiosis will be crucial for ensuring sustainable production and food security[13].

Bradyrhizobium sp. DOA9 was originally isolated from an *Aeschynomene americana* nodule in paddy soil and possesses a unique megasymbiotic plasmid of 736 kb, a rare feature among *Bradyrhizobium* strains[14,15]. DOA9 has the ability to nodulate a wide range of legume plants, with its T3SS playing a crucial role in host interactions. The T3SS has a positive effect on symbiosis with *Stylosanthes hamata* but negatively impacts interactions with *A. hypogaea*, *Crotalaria juncea*, *Macroptilium atropurpureum* and *Vigna radiata*[16]. In silico analysis revealed fourteen putative effectors in the DOA9 genome, including the novel SUMO-like type III effector SkP48, the longest T3E identified to date. SkP48 has been shown to negatively influence the symbiotic interactions of DOA9 with *A. hypogaea*, *C. juncea* and *Vigna* species[17]. The SUMO-protease represents one of the most abundant classes of T3E identified in *Bradyrhizobium* strains. For example, the SUMO-protease Bel2-5 in *B. elkanii* USDA61 can completely inhibit nodulation in *Rj4/Rj4* soybeans[18]. Conversely, the SUMO-protease Sup3 from *Bradyrhizobium* sp. WSM1744, *Bradyrhizobium* sp. ORS86, and *Bradyrhizobium* sp. NAS96.2 has been found to directly activate nodulation in *A.indica*[8]. Additionally, Bel2-5 of USDA61 triggered nodulation in the Nod factor receptor 1 soybean mutant (*nfr1*)[18]. SUMO proteases, also known as desumoylating enzymes, play a critical role in regulating protein function by removing small ubiquitin-like modifier (SUMO) moieties from target proteins. These enzymes are essential components of the dynamic sumoylation system, which allows for rapid and specific modulation of protein activity in response to cellular needs and environmental conditions[19,20]. NopD, a SUMO protease-containing effector from *Bradyrhizobium* sp. XS1150, processes plant SUMO proteins and cleaves SUMO-conjugated substrates, confirming the functionality of its ULP-like domain. These findings support the idea that NopD homologues function similarly to their counterparts in plant pathogens, specifically by deSUMOylating targeted plant proteins[21]. In the genome of *Bradyrhizobium* sp. DOA9, three additional SUMO-proteases (p0490, p0871, and p0903) were identified, although their functions remain unstudied. This study investigated their roles in the symbiotic interaction between DOA9 and *A. hypogaea*. Notably, mutating the SUMO-protease p0903 promoted nodulation in peanuts. The function of the ubiquitin-like protein (ULP) domain in p0903 and the molecular mechanisms underlying the symbiotic interaction mediated by SUMO-protease p0903 were also elucidated in this study.

Results

DOA9 strain displays 4 distinct putative SUMO-protease T3Es

To investigate the relationships among four putative SUMO-proteases identified in DOA9 and other SUMO-proteases from members of the *Bradyrhizobium* genus isolated from legume crops, a phylogenetic tree analysis was conducted (Fig. 1). Two of these SUMO-proteases (p0903 and p0490) forming specific branches in the tree are phylogenetically distant from the other SUMO-proteases used in this analysis. The other two SUMO-proteases belong to two distinct groups: p0873 clusters with 3 other SUMO-proteases identified in strains USDA61 and 1S1, while p0871 clusters a larger group of 5 other SUMO-proteases identified in 3 strains of *Bradyrhizobium*. It thus appears that the 4 SUMO-proteases identified in the DOA9 strain are all phylogenetically distant from each other. This finding indicates that each DOA9 SUMO-proteases may possess specific characteristics and functional roles due to evolutionary divergence. This contrasts with some other *Bradyrhizobium* strains possessing multiple SUMO-proteases, such as the strain *B. septentrionale* 1S1 which has 11 SUMO-protease, 8 of them being clustered together, or the strain *Bradyrhizobium lablabi* CCBAU23086 which has 3 SUMO-proteases which are found also in the same cluster including p0871. It is also to note that the SUMO-proteases from the 3 strains (*B. zhanjiangense* CCBAU51778 and CCBAU51781, and *B. guangdonsense* XS1150) isolated from *Arachis hypogaea* nodules do not group with the DOA9 SUMO-proteases.

Moreover, the domains and structural organization of the four putative SUMO-proteases T3Es from DOA9 were analysed and compared with those of Bel2-5 from USDA61, NopD from XS1150, and XopD from the pathogenic bacterium *Xanthomonas campestris*. All SUMO-proteases share a common ULP-like domain, typically located at the C-terminal (Fig. 2 and Fig. S1). In contrast, the N-terminal regions, which lack functional domains, are highly divergent among proteases. Notably, p0903 and SkP48 each contain two distinct repeat domains (RDs). Although these RDs differ in length and exhibit low amino acid sequence identity, both proteins have unique features. SkP48 includes a shikimate kinase domain and 10 repeat sequences in each RD, whereas p0903 contains RD1 and RD2 sequences without tandem repeat sequences within the RDs. Interestingly, the repeat sequences within RDs from p0903 and SkP48 were significantly different in length and similarity. RD1 and RD2 of p0903 share 94 amino acids, whereas each RD on SkP48 contains 10 repeat sequences that share 41 amino acid conserved sequences (Fig. S2a-d). Additionally, the amino acid sequences of the two RDs of p0903 and the 20 repeat sequences in the two RDs of SkP48 showed complete divergence. This result was confirmed by

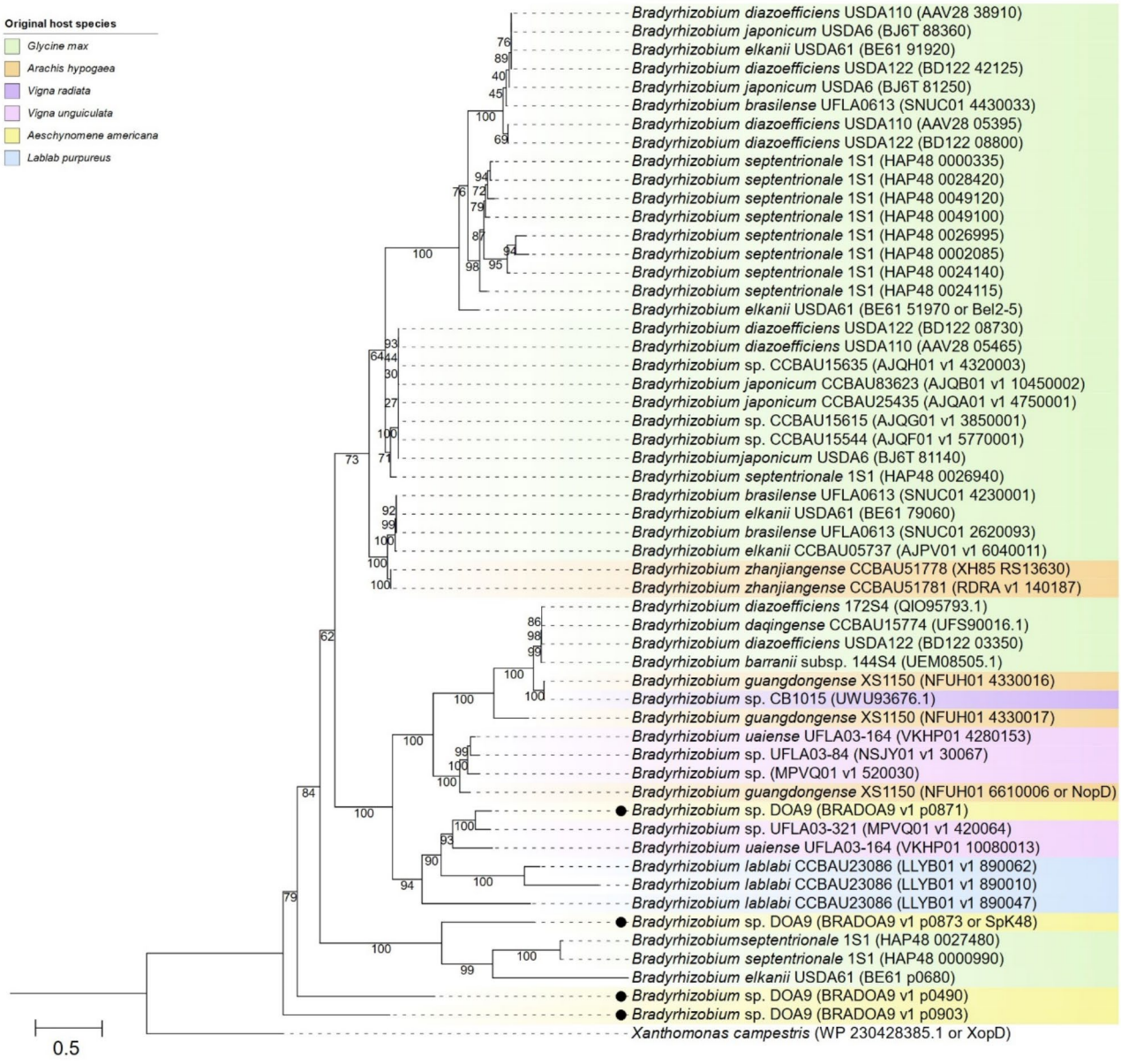

Fig. 1. Phylogenetic tree analysis of four the SUMO-proteases identified in *Bradyrhizobium* sp. DOA9 and other SUMO-proteases from *Bradyrhizobium* species isolated from 6 legume crops indicated in the key. XopD from *Xanthomonas campestris* was used as an outgroup for tree rooting. The GenomeScope and NCBI-derived amino acid sequences of SUMO-proteases were subjected to phylogenetic analyses using IQ-tree v2.2.0.3. The phylogeny was inferred using the maximum-likelihood method, and branch supported with ultrafast bootstrap from 150,000 iterations. The SUMO-proteases from DOA9 were indicated with black dots.

the RADAR graph, which demonstrated that the amino acid composition of the repeat sequences from p0903 and SkP48 was conserved in the separated group (Fig. S2e). Taken together, the strong divergence observed among the four SUMO-proteases identified in the DOA9 strain, which share only the ULP domain while having RDs on p0903 and SkP48 with differing identities, suggests that these putative SUMO-protease T3Es might play distinct roles during the symbiotic interaction of DOA9 with its various legume hosts.

The SUMO-protease p0903 plays a role in peanut symbiosis efficiency

To gain a better understanding of the role of these four putative SUMO-proteases during the symbiosis between DOA9 and peanuts, four delete mutants were constructed via complete gene deletion. All derivative mutant strains were tested on the peanut KK5 cultivar (a commercial shelled peanut that is resistant to necrosis disease[22]) compared with the DOA9 strain and a mutant affected in T3SS machinery secretion (-Ω*rhcN*). Interestingly, we observed that two mutants, DOA9-Δ*p0490* and DOA9-Δ*p0871*, behaved as the DOA9 strain at 30 dpi. They induced a small number of nodules that displayed low nitrogenase activity, and no plant growth benefit was

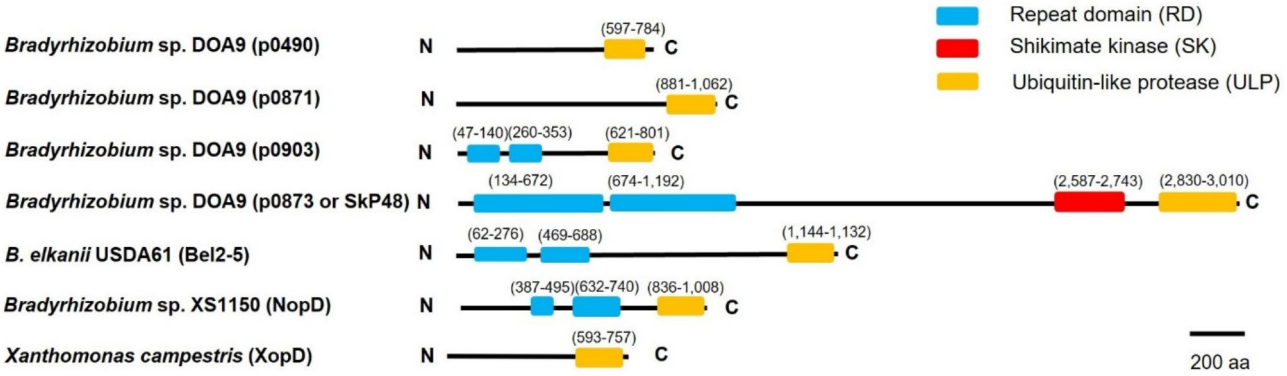

Fig. 2. The structure organization of four-effector proteins containing the small ubiquitin-like modifier (SUMO) protease domain in DOA9 compared with other putative SUMO-proteases among *Bradyrhizobium* species and XopD from pathogenic bacteria *Xanthomonas campestris*. The domain organization includes the repeat domain (blue box), shikimate kinase domain (red box), and ubiquitin-like protease domain (orange box) are shown.

observed (Fig. 3a-c). Furthermore, cytological analysis of the nodules revealed that the infection zone derived from the DOA9, DOA9-Δ*p0490* and DOA9-Δ*p0871* nodules was enriched with dead bacteria (coloured red with PI) (Fig. 3d). In contrast, the other two mutants, DOA9-Δ*SkP48* and DOA9-Δ*p0903*, behave as DOA9-Ω*rhcN*, which increases the nodule number, ARA activity, and plant dry weight. Furthermore, cytological analysis revealed that the infection zone of the nodules is predominantly occupied by living bacteria, which are stained green with SYTO9 (Fig. 3d).

To investigate whether the T3SS in a *Bradyrhizobium* strain originally isolated from *A. hypogaea* plays a role during symbiosis, a T3SS mutant (-Ω*rhcN*) of the type strain *B. arachidis* CCBAU051107 (also named LMG26795) was also constructed and tested on the peanut KK5 cultivar. Observations at 30 dpi revealed that, contrary to what was observed with DOA9, LMG26795 which lacks putative T3Es encoding the SUMO-protease, induced efficient nitrogen-fixing nodules, with no apparent effect of the T3SS mutation (Fig. 3a-d). Interestingly, it is observed that DOA9-Ω*rhcN* and also the DOA9-Δ*p0903* and DOA9-Δ*SkP48* mutants were significantly more efficient in nodulation than LMG26795 (Fig. 3a-d). This suggests that DOA9 could potentially be used as an inoculant for peanut crops if at least one of its incompatible SUMO-protease T3Es (SkP48 or p0903) is deleted. These findings highlight the complex and strain-specific roles of SUMO-protease T3Es in peanut nodulation, with SkP48 and p0903 potentially acting as key modulators of the symbiotic process in certain *Bradyrhizobium* strains.

SUMO-p0903 plays a role in the symbiosis with various peanut cultivars

Considering that SUMO-protease SkP48 was previously investigated in more detail[17], in this study, we focused on the SUMO-protease p0903. To further investigate the role of SUMO-protease p0903 in regulating symbiosis among different cultivars of peanut, two mutants of p0903 (the DOA9-Δ*p0903* deletion mutant and a Δ*p0903* + *p0903* complemented mutant) were inoculated the peanut cultivars TN9, KS2, and SK38. A nodulation test was then performed to compare the results with those of the KK5 cultivar to determine whether p0903 affects other peanut cultivars. As previously observed for the KK5 cultivar, at 30 dpi, DOA9-Δ*p0903* had an increased nodule number per plant in the 3 cultivars tested, which was equivalent to that of DOA9-Ω*rhcN* (Fig. 4a-d). In addition to a greater number of nodules, a gain in symbiotic efficiency (nitrogenase activity, bacterial viability in the nodules, and plant growth) was observed in the plants inoculated with the two DOA9-Δ*p0903* and DOA9-Ω*rhcN* mutants regardless of the peanut cultivars tested (Fig. S3-6). When the *p0903* gene was re-introduced into the DOA9-Δ*p0903* mutant, the complemented strain Δ*p0903* + *p0903* exhibited nodulation patterns similar to the DOA9 strain across four peanut cultivars (Fig. 4a-d). Specifically, it led to a reduction in nodule number, nitrogenase activity, and bacterial viability within nodules (with the exception of TN9 cultivar), as well as overall plant growth. These effects were comparable to those observed in plants inoculated with the DOA9 strain, consistently across all tested peanut cultivars (Fig. S3-6). This restoration of DOA9-like phenotypes in the complemented strain provides strong evidence for the specific role of p0903 in regulating symbiotic interactions.

In addition to Nod factors, rhizobia secrete other molecular signals, such as T3Es, in response to flavonoid compounds released by plant roots[23]. Previous reports have indicated that root exudates from the *A. hypogaea* L. cultivar Tegua contain various flavonoids, such as genistein, daidzein, chrysin, and naringenin[24,25]. To investigate the expression of the SUMO-protease *p0903* gene in DOA9 and *rhcN* gene in LMG26795 under flavonoid induction, pure flavonoids representative of those in peanut root exudates, including control (non-induced), genistein and naringenin, were used (Fig. S7a-b). Compared to the control, the expression of the *p0903* gene was upregulated 3.59-fold when induced with naringenin, but showed no significant difference when induced with genistein (Fig. S7a). These results indicate that naringenin stimulates the expression of the *p0903* gene, while genistein does not have this effect. Furthermore, the T3SS gene (*rhcN*) in LMG26795 was significantly upregulated by both genistein and naringenin compared to the control (Fig. S7b). This result suggests that

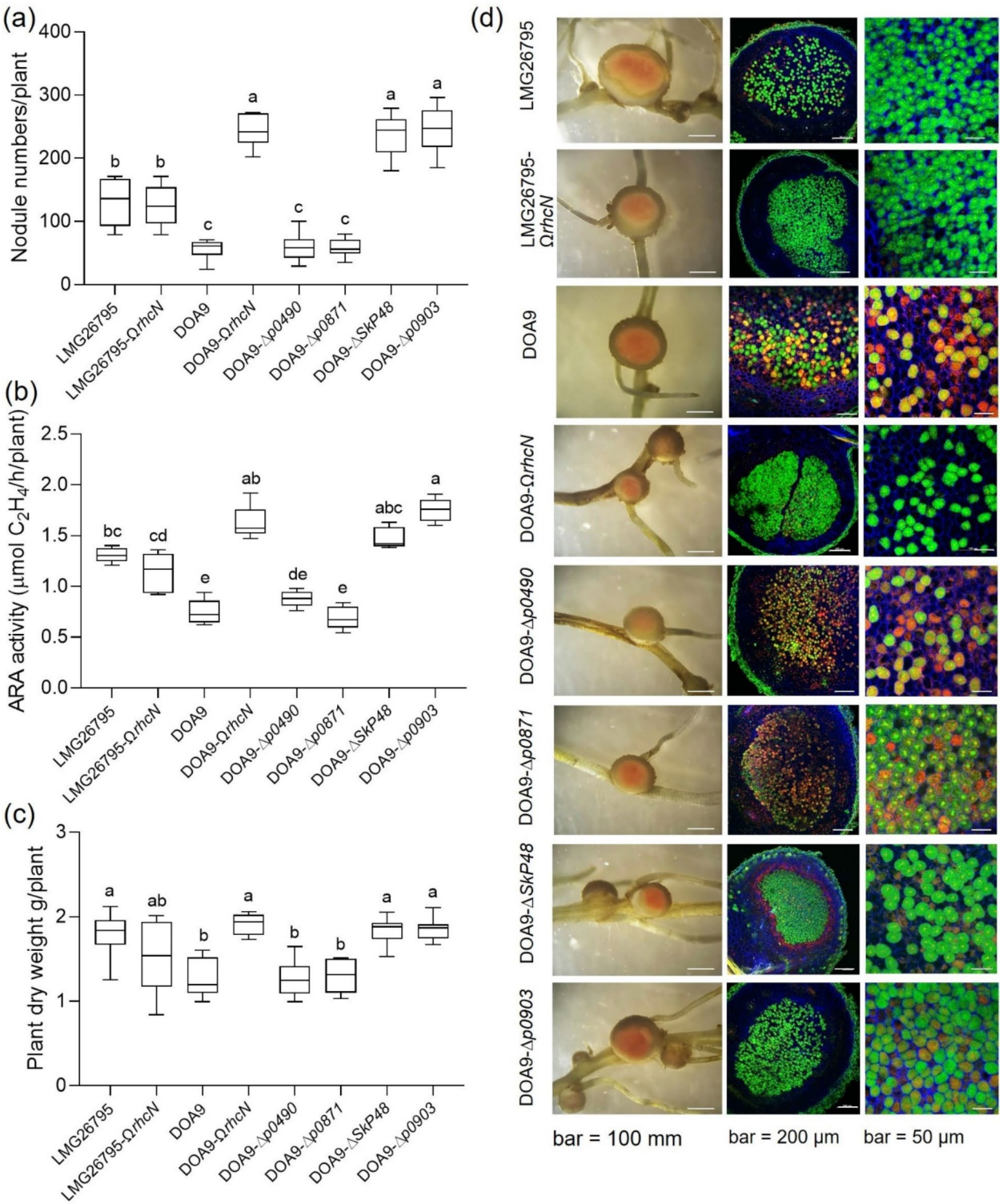

Fig. 3. The symbiotic nodulation of *Bradyrhizobium* sp. DOA9 and its derivative mutants (DOA9-Ω*rhcN*, DOA9-Δ*p0490*, DOA9-Δ*p0871*, DOA9-Δ*p0903*, and DOA9-Δ*SkP48*), as well as *Bradyrhizobium arachidis* LMG26795 and its T3SS mutant (LMG26795-Ω*rhcN*) derivative in peanut (KK5). The assessment at 30 dpi included (**a**) nodule number per plant, (**b**) ARA activity, and (**c**) plant dry weight. The means followed by different letters are significantly different at the 0.1% level ($P \leq 0.001$, according to Tukey's test), with a sample size of $n = 10$, except for ARA activity, where $n = 5$. (**d**) Nodulation in peanut (KK5) manifested as nodules morphology (scale bar: 100 mm), and the nodule sections were stained with SYTO9 (living bacteroid cells: green), propidium iodide (dead bacteroid cells: red), and calcofluor (plant cell wall: blue); scale bar for confocal image: 200 and 50 μm.

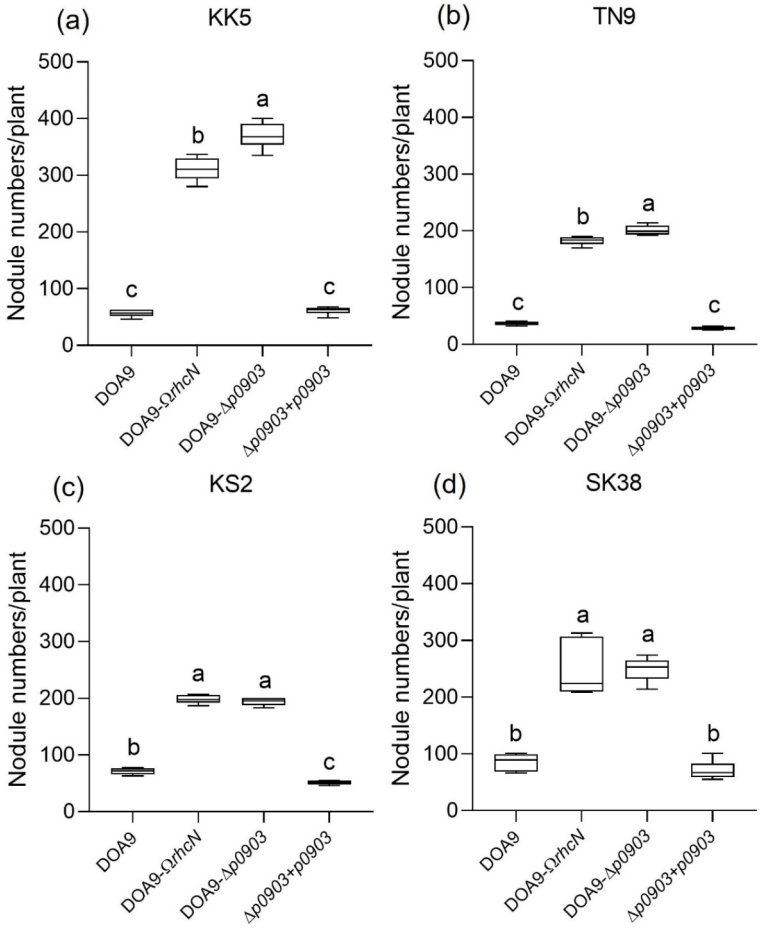

Fig. 4. The symbiotic nodulation of *Bradyrhizobium* sp. DOA9 and its derivative mutants (DOA9-Ω*rhcN*, DOA9-Δ*p0903*, and Δ*p0903* + *p0903*) inoculated in various peanut cultivars (KK5, TN9, KS2, and SK38). (**a**-**d**) The nodule numbers per plant of peanut cultivars (KK5, TN9, KS2, and SK38, respectively) at 30 dpi. The means followed by different letters are significantly different at the 0.1% level ($P \leq 0.001$, according to Tukey's test, with a sample size of $n = 6$).

LMG26795 retains T3SS functionality under symbiotic conditions. However, due to the absence of negative effectors like p0903 in its genome, T3SS mutation does not impact negatively on the symbiotic process.

Taken together, these results indicate that SUMO-protease p0903 induces significant negative effects (less nodules number, weaker nitrogen fixation, and less plant growth benefit) during the symbiotic interaction of the DOA9 strain with the 4 peanut cultivars tested.

The negative symbiotic role of SUMO-protease p0903 is not played only by its ULP domain

The SUMO-protease activity of Bel2-5 from USDA61 and NopD from XS1150 has previously been shown to be important in compromising the symbiotic activity of these two strains on the soybean cultivar BARC-2 (*Rj4*/*Rj4*) and *Tephrosia vogelli*, respectively[18,21]. To investigate whether this is also the case for SUMO-protease p0903 during the symbiotic interaction of DOA9 with *A. hypogaea* KK5, we introduced *p0903* with its native promoter into DOA9-Δ*p0903*. Moreover, variant forms of *p0903*, including two mutants in the catalytic enzymatic core *p0903*-D728A and *p0903*-C763A and the deletion of the complete C-Ter ULP domain, were constructed and independently introduced into DOA9-Δ*p0903* (Fig. 5a). As shown in Fig. 5b, at 30 dpi, the ULP deletion mutant (Δ*p0903* + *p0903*-ULP-lack) and the two point mutation mutants (Δ*p0903* + *p0903*-D728A and Δ*p0903* + *p0903*-C763A) presented an intermediate phenotype in terms of the number of nodules compared with DOA9-Δ*p0903* and DOA9-Δ*p0903* complemented with the wild-type form of *p0903* (Δ*p0903* + *p0903*). However, for the other symbiotic parameters examined, such as chlorophyll content, plant biomass, and ARA nitrogenase activity, no significant differences were detected between these three mutants complemented with mutated forms of ULP and either the DOA9 strain or the DOA9-Δ*p0903* mutant complemented with the wild-type form of *p0903* (Fig. 5c-e). Nonetheless, the viability of infected bacteria in nodules formed by the three mutants complemented with mutated forms of ULP was higher than that observed in nodules induced by either the DOA9 strain or the DOA9-Δ*p0903* mutant complemented with the wild-type *p0903* (Fig. 5f).

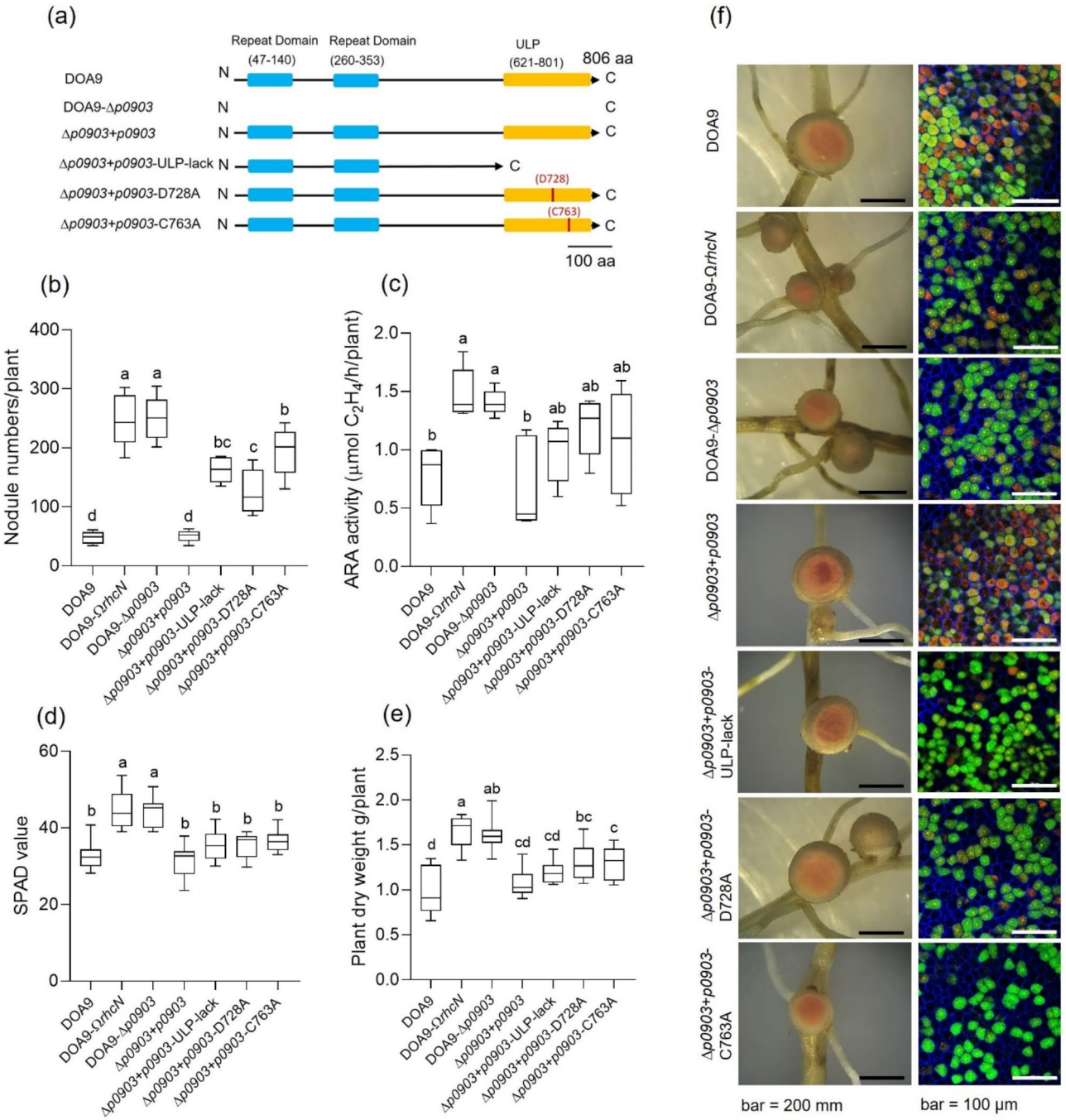

Fig. 5. Nodulation phenotypes of *Bradyrhizobium* sp. DOA9 and its derivatives (DOA9-Ω*rhcN*, DOA9-Δ*p0903*, Δ*p0903* + *p0903*, Δ*p0903* + *p0903*-ULP-lack, Δ*p0903* + *p0903*-D728A, and Δ*p0903* + *p0903*-D763A) on the peanut cultivar (KK5). (**a**) Schematic representation of DOA9 and its mutant derivatives strains. SUMO-protease p0903 possesses two internal repeat domains, a ubiquitin-like protease (ULP) domain, and catalytic core amino acids aspartic acid (D728A) and cysteine (C763A) in ULP domain. Evaluation at 30 dpi included (**b**) nodule count per plant, (**c**) ARA activity, (**d**) chlorophyll content, and (**e**) plant dry weight. The means followed by different letters are significantly different at the 1% level ($P \leq 0.01$, according to Tukey's test), with a sample size of $n = 10$, except for ARA activity, where $n = 5$. (**f**) Nodulation in peanut (KK5) manifested as nodule morphology (scale bar: 200 mm). Nodule sections were stained with SYTO9 (living bacteroid cells: green), propidium iodide (dead bacteroid cells: red), and calcofluor (plant cell walls: blue); scale bar for confocal images: 100 μm.

Taken together, these results suggest that the SUMO-protease activity of p0903 contributes to the negative symbiotic effect observed between strains DOA9 and *A. hypogaea* KK5 but does not explain it on its own; other domains of the protein might also play important roles in this incompatibility.

Gene expression analysis and phytohormone production on peanut root

To investigate the physiological response of plants to SUMO-protease p0903 during symbiosis, the expression of symbiosis-related genes and induced systemic resistance (ISR), which enhances defence against pathogens and microbial symbionts, including jasmonic acid (JA)-related genes, was analysed in plant roots inoculated with DOA9 and DOA9-Δ*p0903*. The expression levels of symbiosis-related genes, including cyclic nucleotide-gated channels (*CNGC*), symbiotic remorins (*SYMREM*), and the E3 ubiquitin-protein ligase LIN-1 (*CERBERUS*), at 3 dpi are depicted in Fig. 6a. These three symbiosis-related genes were downregulated in the DOA9 plants compared with those in the DOA9-Δ*p0903*-inoculated plants. Furthermore, the expression levels of JA-related genes, including a transcription factor (*Myc2*), pathogenesis-related protein (*PR4*), and defensin (*Def2-2*), are presented in Fig. 6b. The expression levels of *Myc2*, *PR4*, and *Def2-2* were significantly increased in the DOA9 plants than in the DOA9-Δ*p0903*-inoculated plants. These results suggest that SUMO-protease p0903 in DOA9 might suppress the expression of symbiosis-related genes while triggering the expression of JA-related genes.

To understand the role of SUMO-protease p0903 in stimulating the accumulation of JA in peanut KK5 roots, the concentration of JA was measured (Fig. 6c). The treatments included non-inoculated (NI), DOA9, DOA9-Δ*p0903*, and Δ*p0903* + *p0903*-ULP-lack. At 3 dpi, JA acid production in peanut roots was 2.32-, 1.27-, and 0.64-fold greater in DOA9, DOA9-Δ*p0903*, and Δ*p0903* + *p0903*-ULP-lack, respectively, than in non-inoculated plants, with a JA concentration of 49.56 µg/g root fresh weight. The results show that the ULP domain induces JA accumulation in peanut roots in a manner similar to that of p0903. These results indicate that SUMO-protease p0903 plays a role in triggering the production of JA to induce JA-related genes in peanut roots, thus suppressing crucial symbiosis-related genes at the early stages of peanut nodulation with *Bradyrhizobium* sp. DOA9.

Discussion

In the process of nodulation, peanuts utilize NF-dependent mechanisms for nodulation[26]. The T3SSs of *Bradyrhizobium* sp. DOA9 and *Bradyrhizobium* sp. MM6 play a negative role in symbiosis with peanuts[16,27]. Our results also demonstrated that the T3SS of DOA9 suppresses nodulation in the peanut KK5 cultivar (Fig. 3a-d). In contrast, the T3SS of *B. arachidis* LMG26795, a peanut-nodulating strain, does not significantly impact nodulation in the peanut KK5 cultivar. Similarly, for *B. zhanjiangense* CCBAU51778, a peanut-nodulating strain, the T3SS is not important for nodulation[28]. The results suggest that the T3SS of bradyrhizobia might play either a negative role or has no effect on peanut symbiosis with the KK5 peanut cultivar, depending on the host specificity of the *Bradyrhizobium* strains. This implies that while peanut-associated *Bradyrhizobium* strains have likely evolved to minimize the negative impact of the T3SS on their host, strains from other plants might retain certain T3SS effectors that could disrupt symbiosis with peanuts. Therefore, for the development of a *Bradyrhizobium* inoculant that would be efficient on a wide range of cultivated host plants, including peanut, the selection or engineering of *Bradyrhizobium* strains that lack either T3SS or incompatible T3SS effectors is crucial.

In DOA9, four putative SUMO-proteases T3Es, p0490, p0871, SkP48, and p0903, were identified (Fig. 1). Mutagenesis analysis of these four SUMO-proteases indicates that SkP48 and p0903 restricted nodulation in peanuts (KK5), whereas SUMO-proteases p0490 and p0871 had no effect on peanut nodulation (Fig. 3a-d). The fact that the mutation of either *SkP48* or *p0903* promote nodulation, at a level similar than of the *rhcN* mutant, suggest that these two SUMO-proteases might act in tandem and that a combined action of these two T3Es is required to impeded the symbiosis. Analysis of a double mutant, currently underway, should provide a better understanding of how the action of these 2 effectors combine to repress symbiosis. In addition, it would be interesting to study whether these two SUMO-proteases target the same plant proteins and investigate whether the repeat domains (RDs) identified in these proteins contribute to this targeting.

There are several other reports indicating that some SUMO-protease T3Es identified in various *Bradyrhizobium* strains can restrict nodulation in other legume crops[18,21,29]. Furthermore, several strains of bradyrhizobia isolated from effective nodules of peanut[30] (*B. zhanjiangense* CCBAU51778 and *B. zhanjiangense* CCBAU51781) contain T3Es with ULP domains (Fig. 1). In contrast, other strains (*B. arachidis* LMG26795 and *Bradyrhizobium* sp. SEMIA6144) isolated from peanuts lacked T3Es containing a ULP domain. Notably, these latter strains are considered good inoculants for increasing peanut yield[26,27]. Interestingly, it is observed that DOA9-Ω*rhcN* and also the DOA9-Δ*p0903* and DOA9-Δ*SkP48* mutants were significantly more efficient in nodulation than LMG26795 (Fig. 3a-d). This suggests that DOA9 could potentially be used as an inoculant for peanut crops if at least one of its incompatible SUMO-protease T3Es (SkP48 or p0903) is deleted. These findings highlight the complex and strain-specific roles of SUMO-protease T3Es in peanut nodulation, with SkP48 and p0903 potentially acting as key modulators of the symbiotic process in certain *Bradyrhizobium* strains. Therefore, selecting compatible SUMO-protease T3Es in *Bradyrhizobium* for peanut inoculant production is crucial to promote plant growth.

Naringenin, a flavonoid found in legumes, plays a significant role in the symbiotic relationship between rhizobia and legume plants[31]. This flavonoid is known to activate nodulation genes in rhizobia by binding to the NodD transcriptional activator. This binding triggers the expression of *nod* gene, leading to the production of Nod factors that initiate the formation of root nodules where nitrogen fixation occurs[32–34]. Naringenin has been reported to be expressed in peanut roots[35]. Furthermore, under water deficit conditions, naringenin present in the root exudates of peanuts enhances bacterial mobility, chemotaxis, and adhesion to the roots[25]. Interestingly, the expression level of the *rhcN* gene in DOA9 is induced by naringenin and peanut root exudates[16]. Furthermore, flavonoids were shown to stimulate the expression of several T3Es in *Bradyrhizobium* sp[36,37]. In accordance, we

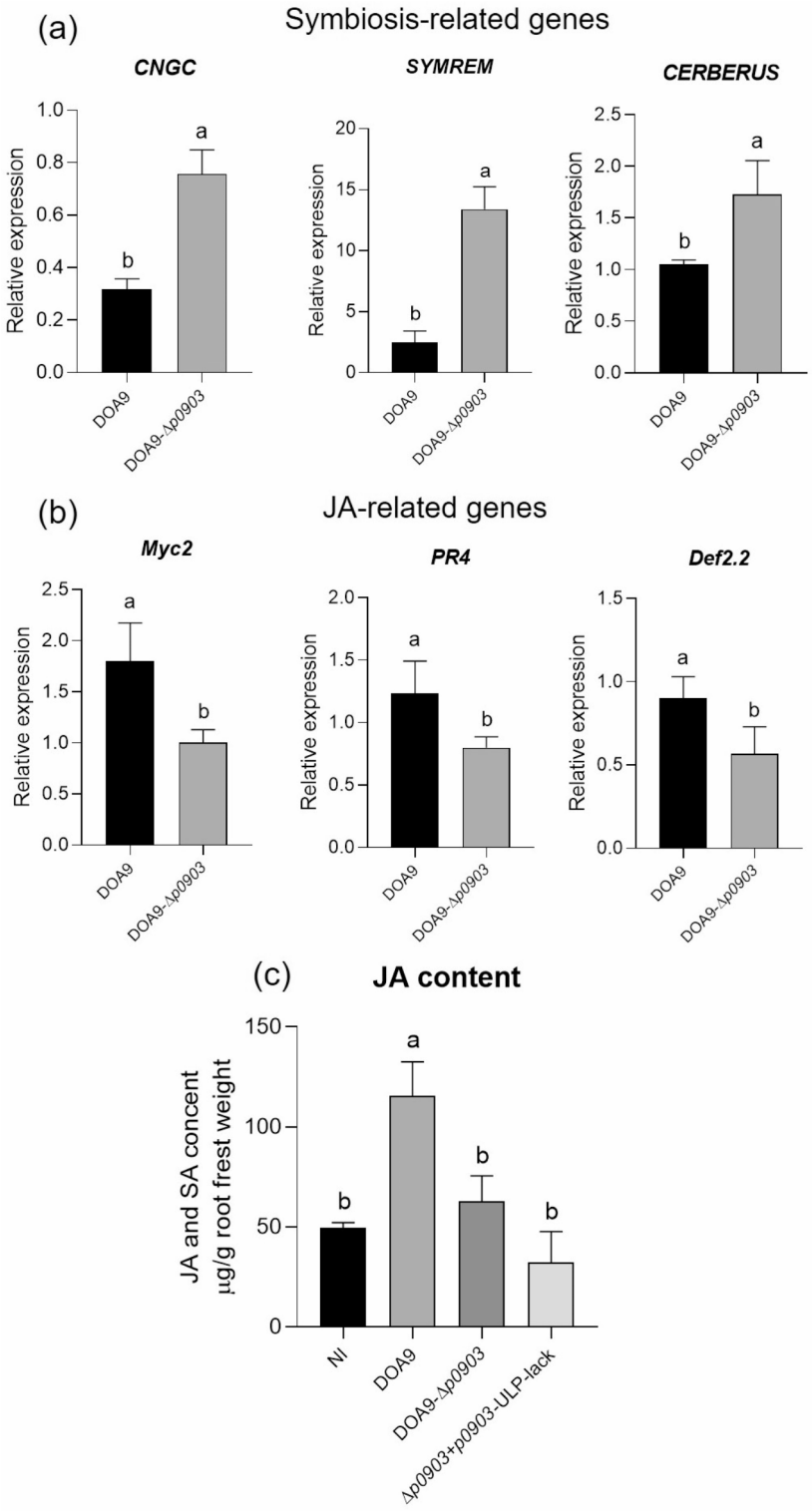

Fig. 6. qRT-PCR results of gene expression and jasmonic acid levels in peanut roots (KK5). The relative expression levels of genes in peanut roots inoculated with DOA9 and DOA9-Δ*p0903* at 3 dpi are shown for: (**a**) symbiotic-related genes (cyclic nucleotide-gated channels [*CNGC*], symbiotic remorins [*SYMREM*], and E3 ubiquitin-protein ligase LIN-1 [*CERBERUS*]); (**b**) jasmonic acid (JA)-related genes (transcription factor [*Myc2*], pathogenesis-related protein 4 [*PR4*], and defensin [*Def2-2*]). The means followed by different letters are significantly different at the 5% level ($P \leq 0.05$, according to Student's t-test, with a sample size of $n = 3$). (**c**) Jasmonic acid concentrations in peanut roots for the following treatments: Non-Inoculated (NI), DOA9, DOA9-Δ*p0903*, and Δ*p0903* + *p0903*-ULP-lack at 3 dpi. The means followed by different letters are significantly different at the 1% level ($P \leq 0.01$, according to Tukey's test, with a sample size of $n = 3$).

observed that naringenin induces also the expression of the putative T3E-*p0903* in DOA9, whereas genistein is less important (Fig. S7a). We showed also that the addition of genistein and naringenin induced *rhcN* expression in LMG26795 (Fig. S7b). These results are in line with previous studies showing that T3SS and T3Es expression in other *Rhizobium* strains is dependent on these two flavonoids[32,38]. Given that these two flavonoids were detected in the root exudates of *A. hypogaea*[24,25], we can assume that the T3SS of LMG26795 is functional during symbiosis and permits the translocation of T3Es in *A. hypogaea* cells. LMG26795 contains several T3Es, such as NopP, NopL and NopT, but lacks T3E SUMO-proteases, which may explain why we did not observe a negative role of T3SS in LMG26795 strain during interaction with *A. hypogaea*.

Interestingly, we observed that the SUMO-protease p0903 restricted nodulation in three other peanut cultivars (TN9, KS2, and SK38), similar to its effect on KK5 (Fig. 4a-d and Fig. S3-6). These results suggest that SUMO-protease p0903 might interact with homologous genes in peanut cultivars to affect symbiotic nodulation. Furthermore, in yeast cells, ULP1 plays a role in the SUMO modification pathway, with dual functions of processing the SUMO precursor into mature SUMO and removing SUMO from its substrate protein[39]. The catalytic amino acid C1268A within the ULP domain of Bel2-5 plays a critical role in suppressing nodulation in soybean BARC-2 (*Rj4/Rj4*)[18]. In addition, NopD-C972A in XS1150 resulted in nodulation suppression similar to that of the full-length *NopD* gene in *T. vogelii*[21]. The SUMO-protease p0903 on DOA9 contained the H/G/C catalytic triad residues within the ULP-like domain, similar to XopD of *X. campestris* (Fig. S1). In this study, the deleted ULP mutant as well as the D728A, and C763A mutants restricted nodule numbers in the peanut cultivar KK5 but not to the same level as the DOA9 (Fig. 5b). In contrast, they did not induce bacteroid cell death in nodules, similar to DOA9 (Fig. 5f). This result suggests that the restriction of nodulation in *A. hypogaea* induced by the SUMO-protease p0903 do not result only to the SUMO-protease activity of the ULP domain but also to an effect of the N-terminal region. This one contains two repeat domains (RD). The presence of RD has been reported in several SUMO-proteases from pathogenic and symbiotic bacteria and shown to modulate the interaction with the host plants. This is the case of the pathogenic T3E HsvG identified in *Pantoea agglomerans* which features tandem repeats of 71 and 75 amino acids that were shown to serve as transcriptional activator and influence host specificity[40]. A similar repeat sequence was identified in *Ralstonia solanacearum* T3E RipTAL1, which is known for activating the transcription of host susceptibility genes[41]. In the symbiotic strain *B. elkanii* USDA61 strain, the deletion of the two RDs in the SUMO-protease Bel2-5 restricted nodulation to soybean BARC-2 *(Rj4/Rj4)*, similar to the deletion of Bel2-5[18]. It is therefore tempting to suggest that the symbiotic incompatibility provoked by the SUMO-protease p0903 during the interaction of DOA9 and various peanuts result to a combined effect of the ULP and RD domains. Transcriptome analysis of early nodulation phases between peanut and *Bradyrhizobium* sp. SEMIA6144 revealed the involvement of early symbiotic signalling genes, including cyclic nucleotide-gated channels (*CNGC*), symbiotic remorins (*SYMREM*), and the E3 ubiquitin-protein ligase LIN-1 (*CERBERUS*)[42]. Our study revealed that the expression levels of these 3 genes were lower in the DOA9 than in DOA9-Δ*p0903* (Fig. 6a). *CNGC* are regulated by the calcium-bound form of calmodulin 2 (holo-CaM2) to modulate *CNGC* activity and the downstream root nodule symbiosis pathway[43]. Furthermore, *SYMREM 1* from *Medicago truncatula* interacts with various symbiotic receptor kinases, including *LYK3* and *SymRK*, potentially serving as a scaffold protein for assembling signalling complexes crucial for rhizobial infection[44]. Additionally, *LjCERBERUS* encodes a novel protein containing a U-box domain and WD-40 repeats, which produces more prenodule structures in response to rhizobium infection and controls plant defence response pathways[45,46]. These results suggest that SUMO-protease p0903 might be involved in suppressing early symbiosis-related genes to reduce the number of bacterial infections.

Rhizobial invasion of plant roots can trigger an increased systemic resistance state in the host, resembling the induced systemic resistance (ISR) mechanism, which includes JA plant defence signalling[47]. Additionally, *Myc2* orchestrates a hierarchical transcriptional cascade that regulates jasmonate-mediated plant immunity[48]. Pathogen-related protein 4 (*PR4*) genes are induced by activators of systemic acquired resistance and wounding[49]. Moreover, defensins play a role in plant immune responses via the JA signalling pathway[50]. Previous reports have shown that NopE of *B. diazoefficiens* USDA110 triggers the expression of the *defensin* gene to manage nodulation compatibility with *V. radiata* KPS2[51]. Our results indicate that SUMO-protease p0903 triggers the expression of JA-related genes (*Myc2*, *PR4*, and *Def2-2*) in peanut KK5 (Fig. 6b). This is correlated with an accumulation of JA in the roots inoculated with DOA9 in comparison to the roots inoculated with the DOA9-Δ*p0903* mutant (Fig. 6c). These findings suggest that SUMO-protease p0903 might stimulate JA production, thereby inducing a defence response to inhibit early nodulation in peanut roots.

To optimize the use of rhizobium (or *Bradyrhizobium*) inoculants, it is essential to identify genetic determinants that affect symbiotic relationships with peanut plants. One such determinant is the SUMO-protease, which plays a significant role in the regulation of symbiotic interactions. Understanding how the SUMO-protease influences symbiosis can guide the development and selection of the most effective inoculant strains. This knowledge will allow the creation of tailored inoculants that maximize peanut productivity and support sustainable agricultural practices.

In conclusion, naringenin has been shown to play a crucial role in the symbiotic interaction between *Bradyrhizobium* sp. DOA9 and peanut plants. This compound induces the transcription of nodulation (*nod*) genes in DOA9 as well as the T3SS and T3Es genes. The T3SS then permits the secretion of T3Es, such as the SUMO-protease p0903, into the root cells of the peanut cultivar KK5. The peanut KK5-mediated incompatible interaction between peanut and DOA9 involves the accumulation of JA and the induction of defence genes (*Myc2*, *PR4*, and *Def2-2*), similar to the case of effector-triggered immunity (ETI). These findings imply that SUMO-p0903, when recognized by the host surveillance system, triggers a phytohormone-mediated effector-triggered immunity type (PmETI type) that suppresses early symbiotic genes (*CNGC*, *SYMREM*, and *CERBERUS*) and strongly inhibits rhizobial infection (Fig. 7). This study reveals a shared molecular mechanism in both plant–pathogen and plant–symbiont interactions, indicating that the reduction in root nodule symbiosis is triggered by plant immune responses to rhizobial effectors.

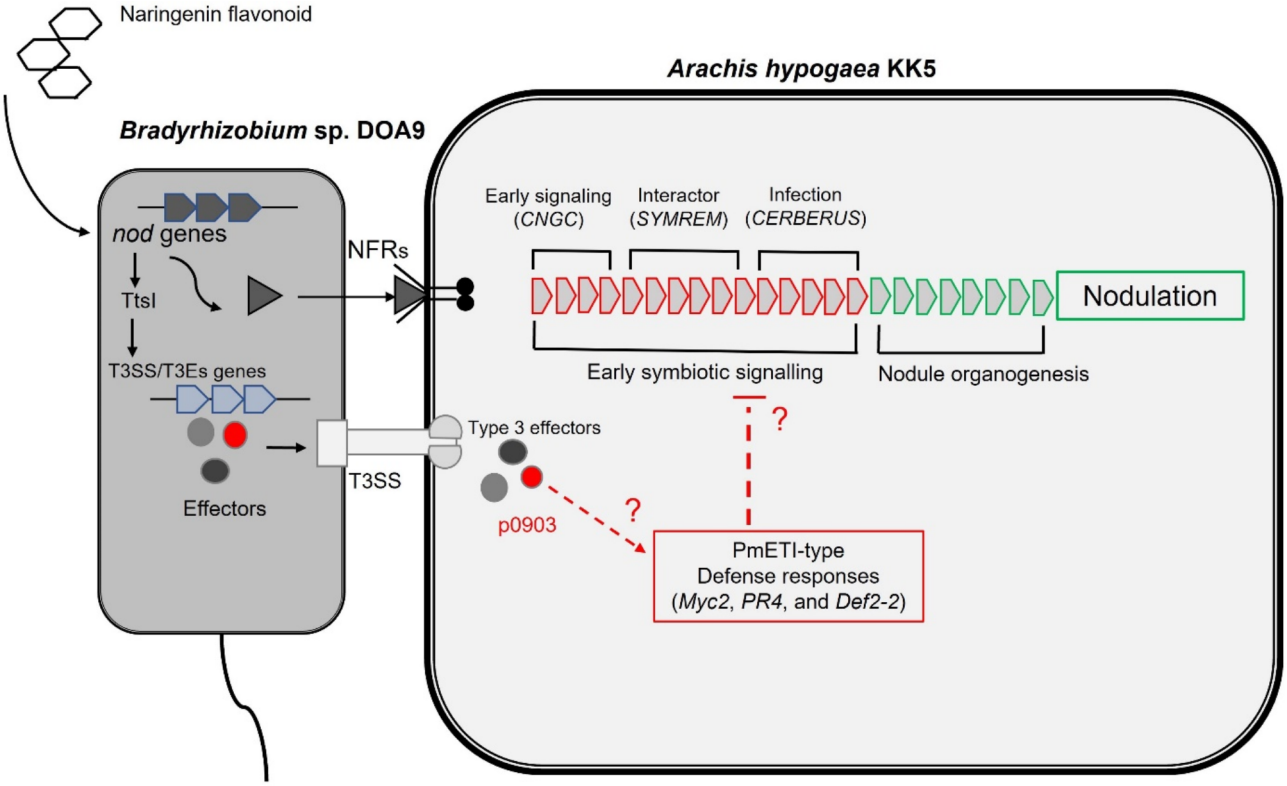

Fig. 7. Schematic overview of the putative SUMO-protease p0903 T3E symbiotic process between *Bradyrhizobium* sp. DOA9 and peanut (KK5). Theoretically naringenin induces the expression level of the putative T3E-*p0903* gene. Consequently, SUMO-protease p0903 might trigger phytohormone-mediated effector-triggered immunity (PmETI-type) genes, including transcriptional factor (*Myc2*), pathogenesis-related protein 4 (*PR4*), and defensin (*Def2-2*), to block early infection. Additionally, SUMO-protease p0903 is a key regulator of early symbiosis signalling in peanuts (KK5), influencing genes involved in various stages of early signalling such as cyclic nucleotide-gated channels (*CNGC*), symbiotic remorins (*SYMREM*), and E3 ubiquitin-protein ligase LIN-1 (*CERBERUS*). The dotted line indicates the unclear symbiotic mechanism.

Materials and methods

Bacterial strains and growth conditions

The bacterial mutants of *Bradyrhizobium* sp. DOA9 used in this study are summarized in Table S1. DOA9 and the derivative mutants were subsequently grown in yeast mannitol (YM) media or arabinose-gluconate (AG) media at 28 °C[52,53]. *Escherichia coli* strains XL2-Blue (Agilent) and S17-1 were cultured in Luria–Bertani (LB) media at 37 °C[54]. When needed, the media were supplemented with the following antibiotic concentrations: 20 µg/mL nalidixic acid (Amresco); 20 µg/mL cefotaxime, Cefo (GoldBIO); 50 µg/mL kanamycin, Km (BIO BASIS); and 200 µg/mL spectinomycin, Sm (Glentham).

Plasmid construction, mutagenesis, and complementation

The deletion mutants of DOA9-Δ*p0490*, DOA9-Δ*p0871*, and DOA9-Δ*p0903* were constructed via a double homologous recombination method. To achieve this goal, PCR fragments of approximately 750-1,000 base pairs corresponding to the regions flanking each gene were combined via overlap extension PCR (primer Table S2 and construction map Fig. S8). The cloning sites of the *p0490* and *p0871* genes were *Eco*RI/*Bam*HI (Enzyme: Thermo Scientific), whereas the *p0903* gene was *Xba*I (Enzyme: Thermo Scientific) and *Bgl*II (Enzyme: NEB). After overlapping the PCR products, they were ligated into the pK18mob-*sacB-cefo* plasmid[55]. In addition, the recombinant plasmids were introduced into *E. coli* S17-1 and then transferred into DOA9 via conjugation, followed by biparental mating. The selection of these recombinants was carried out following previously established protocols[56].

For the complementation Δ*p0903* + *p0903* strain, a DNA fragment of 2,532 bp containing the *p0903* gene along with its promoter sequence and an 8xHis tag before the stop codon was used. PCR was performed via specific primers, as indicated in Table S2, and the resulting map is shown in Fig. S8. The restriction site was *EcoR*I/*Sal*I (Enzyme: Thermo Scientific), which was subsequently ligated into the pMG103-*npt2-cefo* plasmid[57]. The recombinant plasmid (pMG103-*p0903-8xHis-npt2-cefo*) was introduced into the DOA9-Δ*p0903* strain through electroporation (17.5 kv/cm, 100 Ω, and 25 µF)[58]. The PCR products were verified and selected.

To complement the Δ*p0903* + *p0903*-ULP-lack domain, a 1,778-bp fragment of the *p0903* gene lacking the ULP domain was PCR-amplified via the specific primers detailed in Table S2. The construction map is shown

in Figure S8. The *Sal*I (Enzyme: Promega) restriction site was used for cloning the PCR product. The inserted gene was subsequently integrated into pMG103-*npt2-cefo-npt2-gfp*. The complementation construct plasmid was then introduced into the DOA9-Δ*p0903* strain via electroporation. The mutant was selected on YM media supplemented with antibiotics, confirmed via PCR, and chosen as previously described[58].

For the site-directed mutagenesis of Δ*p0903* + *p0903*-D728A and Δ*p0903* + *p0903*-C763A, the plasmid pMG103-*p0903-8xHis-npt2-cefo* was used for construction, as indicated by the construction map in Fig. S8. This process was performed with the Q5 Site-Directed Mutagenesis Kit (NEB) along with the primers listed in Table S2 for PCR amplification[8]. PCR was conducted to introduce changes in the amino acids D728A and C763A, substituting them with alanine residues[21]. The PCR product was subsequently ligated for construction of the plasmid. The recombinant plasmid was then electroporated into the DOA9-Δ*p0903* strain. Mutants were selected on YM media supplemented with antibiotics and verified via PCR as described previously[58].

Peanut nodulation and symbiosis analysis

The 4 genotypes of *Arachis hypogaea*that were tested are Thai published varieties that are normally cultivated by Thai farmers (KK5, TN9, KS2, and SK38) (Table S3). This study complies with local and national regulations in Thailand. The seeds of the peanut cultivars were washed in 70% ethanol for 30 s and then rinsed once with sterile water. The samples were subsequently subjected to surface sterilization with a 3% (v/v) sodium hypochlorite solution for 30 s, followed by five washes in sterilized water. After being germinated on vermiculite for 3 days, the seedlings were transplanted into Leonard jars filled with vermiculite and watered with BNM[59]. The plants were cultivated under controlled environmental conditions: 28 °C with a 16-hour light and 8-hour dark cycle at light intensities of 300 µmol/m^2 s and 70% humidity. DOA9, LMG26795, and their derivatives were grown in YM media at 30 °C for five days. At 5 days, each seedling was inoculated with 1 mL of a 5-day-old inoculum, adjusted to an optical density at 600 nm of 1 (approximately 10^9cells/mL), and washed with sterilized water before use. At 30 dpi, the leaf chlorophyll content was measured via a Minolta SPAD-502 chlorophyll meter, the number of nodules was counted, and the dry weight of the plants was noted. Additionally, living and dead bacteroid cells were observed via confocal microscopy. Finally, an acetylene reduction assay (ARA) was performed as described previously[60].

Analysis of the function of SUMO-p0903 in peanut cultivar symbiosis

The nodulation test followed the same procedure as described above for growth conditions and data collection. The peanut cultivars used in this study are listed in Table S3. Each treatment consisted of six replicates, including the wild type (DOA9), *rhcN* insertion mutant strain (DOA9-Ω*rhcN*), *p0903* deletion mutant strain (DOA9-Δ*p0903*), and *p0903* complementation mutant strain (Δ*p0903* + *p0903*).

Analysis of the effects of the ULP domain on peanut K55 cultivar symbiosis

The peanut cultivar KK5 was used for the symbiotic test. The treatments included DOA9, DOA9-Ω*rhcN*, DOA9-Δ*p0903*, Δ*p0903* + *p0903*, ULP domain deletion mutants of *p0903* (Δ*p0903* + *p0903*-ULP-lack), D728A point mutation of *p0903* (Δ*p0903* + *p0903*-D728A), and C763A point mutation of *p0903* (Δ*p0903* + *p0903*-C763A) strains. The plant conditions and data collection followed the same protocol used for the nodulation test described earlier. The data collection consisted of ten replications, with the exception of five replications for the ARA measurement.

Microscopy

An Olympus Fluoview FV1000 confocal laser scanning microscope (Japan) was used to examine the bacteroid morphology. Nodule sections, approximately 33–40 µm thick, were prepared using a Leica vibratome (VT1000S; Nanterre, France). The bacteria were treated with a live/dead staining solution comprising 5 µM SYTO9 (Invitrogen) and 30 µM propidium iodide (Invitrogen) in 50 mM Tris-HCl (pH 7.0) and incubated for 15 min. Following staining, the sections were washed with 10 mM phosphate saline buffer. For an additional 5 min, the plant cell walls were stained with calcofluor white M2R (Sigma) at a final concentration of 0.01% (w/v). The chemicals present in the nodule stain were excited to detect the presence of live bacteroids via a previously described method[61]. Cytological analysis of nodules was performed using a Nikon Eclipse Ti-E Inverted Confocal Laser Scanning Microscope (Tokyo, Japan) to visualize nodule development and assess bacteroid viability within symbiosomes.

Bacterial RNA extraction and expression analysis

The mid log phase cultures of DOA9 and LMG26795 were washed, and their $OD_{600}$was adjusted to approximately 0.4 using AG medium supplemented with purified flavonoids (20 µM genistein and naringenin dissolved in DMSO) from Sigma. DMSO alone served as the negative control. The bacterial cells were subsequently cultured at 28 °C for 24 h and harvested via centrifugation (4,000 rpm for 10 min at 4 °C). Total bacterial RNA was extracted from the induced cells via the previously described manure method[62]. The extracted RNA was treated with RNase-free DNaseI (NEB) for 30 min at 37 °C. The purity and concentration of RNA were measured via a NanoDrop, resulting in A260/280 and A260/230 ratios of 2.1 and 2.1 to 2.4, respectively. cDNA was subsequently synthesized from 500 ng of total RNA via the High-Capacity cDNA Reverse Transcription Kit (iScript, Bio-Rad) according to the manufacturer's protocol. Next, the synthesized cDNA (50 ng) was used for PCR amplification with gene-specific primers (Table S4) via the CFX Opus 96 Real-Time PCR System (Bio-Rad, USA). The PCR program consisted of an initial denaturation step at 95 °C for 2 m, followed by 40 cycles at 95 °C for 30 s, 60 °C for 30 s, and 72 °C for 30 s. To analyse gene expression, the comparative Ct ($^{-\Delta\Delta CT}$) method was used[63], and the data were normalized to the expression of the endogenous housekeeping gene 16 S rRNA (primer: PBA338F/PRUN518R). The analysis was based on data obtained from three biological replicates, and at least three PCR amplifications were performed for each sample.

Gene expression analysis of peanut KK5

The peanut seeds were surface sterilized, germinated, and grown under the same conditions as those described above for the nodulation test. The seedlings were inoculated with DOA9 or DOA9-Δ*p0903*. At 3 dpi, the peanut roots were frozen in liquid nitrogen and ground into a fine powder, and 100 mg of the powder was used for total RNA extraction via the FavorPrep Plant Total RNA Mini Kit (Favorgen). The RNA purification followed the same procedure as described above. The RNA samples were then converted into cDNA from 1,000 ng of total RNA via the High-Capacity cDNA Reverse Transcription Kit (iScript, Bio-Rad) according to the manufacturer's protocol. Then, a 10-fold dilution of cDNA was used with specific primers (Table S4) for amplification of each gene. The qRT-PCR conditions were the same as those described above. Relative gene expression was calculated via the Ct ($^{-\Delta\Delta CT}$) method[63]. To normalize the transcript levels of the sample genes, the expression of the β-actin gene was measured in the same samples.

Measurement of jasmonic acid content in peanut root

At 3 dpi, the peanut roots were harvested and ground to a fine powder in liquid nitrogen. Subsequently, 100 mg of the powder was mixed with 1 mL of 90% methanol, homogenized for 2 min at 6,000 rpm, and then incubated overnight at 4 °C. The mixture was centrifuged at 1,200×g for 10 min at 4 °C, and the supernatant was collected, freeze-dried, and resuspended in 400 µL of 1 M trichloroacetic acid. This suspension underwent three partitioning steps against hexane: ethyl acetate 200 µL (1:1), with the organic phase collected and freeze-dried. The sample extract, standard jamonic acid (Glentham), was dissolved in 1000 µL of methanol, filtered through a 0.22-µm PTFE membrane, and prepared for analysis via triple quadrupole LC–MS/MS (AB Sciex QTRAP 6500 LC–MS/MS platform). The separations were performed on a Thermo Scientific ™ Acclaim ™ 120 C18 column (100 mm × 2.1 mm, 2.2 µm). The HPLC conditions and gradient were used for all analyses, which took 13.6 min. The injection sample volume was 5 µL and consisted of mobile phases A (formic acid in water with 0.1% (v/v)) and B (acetonitrile). The gradient time frame was as follows: 0 min 10% A; 1 min 10% A; 2 min 40% A; 7 min 95% A; 9 min 95% A; 9.1 min 10% A; and 13.6 min 10% A. The column compartment was heated to 35 °C.

Phylogenetic tree and in silico protein analysis

The MicroScope and NCBI platforms were used to search for the amino acid sequence SUMO T3Es of all strains, which are accessible at http://www.genoscope.cns.fr/agc/microscope[64] and https://www.ncbi.nlm.nih.gov/protein/. A phylogenetic tree was subsequently constructed using IQ-tree v2.2.0.3[65] based on an alignment of the selected SUMO-proteases protein sequences using ClustalW (http://www.clustal.org/omega/). The phylogeny was inferred from the resulting alignment under the model recommended by ModelFinder[66]and branch supports with ultrafast bootstrap were estimated from 150,000 iterations[67]. Additionally, repeat domain analysis of SUMO-proteases p0903 and SkP48 from DOA9 was conducted via WebLogo and Microsoft Excel 2010. WebLogo (accessible at https://weblogo.berkeley.edu/logo.cgi) was utilized to generate graphical representations of the repeat sequences (RSs) within the repeat domain alignments of SUMO-proteases p0903 and SkP48. A radar graph created via Microsoft Excel 365 was used to construct a spider map of the RSs of SUMO-proteases p0903 and SkP48.

Statistical analysis

Data analysis was conducted using SPSS software (version 26.0 for Windows; SPSS Inc., Chicago, IL) to verify the statistical significance of the ANOVA results. Tukey's HSD test was employed as a post hoc test for the plant test analysis and jasmonic acid analysis, with significance levels set at $P \leq 0.05$, $P \leq 0.01$, and $P \leq 0.001$. qRT-PCR analysis was performed, and a two-tailed Student's t-test was applied for pairwise comparisons. Statistical significance was set at $P \leq 0.05$. Detailed information on sample size and replicates is provided in the figure and table legends.

Data availability

All data produced or analyzed in this study are available in this published article and its Supplementary Information files.

Received: 4 August 2024; Accepted: 5 November 2024
Published online: 30 December 2024

References

1. Prakamhang, J. et al. Proposed some interactions at molecular level of PGPR coinoculated with *Bradyrhizobium diazoefficiens* USDA110 and *B. Japonicum* THA6 on soybean symbiosis and its potential of field application. *Appl. Soil. Ecol.* **85**, 38–49 (2015).
2. Vicario, J. C., Primo, E. D., Dardanelli, M. S. & Giordano, W. Promotion of peanut growth by co-inoculation with selected strains of *Bradyrhizobium* and *Azospirillum*. *J. Plant. Growth Regul.* **35**, 413–419 (2016).
3. Ayalew, T., Yoseph, T., Petra, H. & Cadisch, G. Yield response of field-grown cowpea varieties to *Bradyrhizobium* inoculation. *Agron. J.* **113**, 3258–3268 (2021).
4. Teulet, A. et al. The rhizobial type III effector ErnA confers the ability to form nodules in legumes. *Proc. Natl. Acad. Sci.* **116**, 21758–21768 (2019).
5. Okazaki, S. et al. Rhizobium–legume symbiosis in the absence of nod factors: two possible scenarios with or without the T3SS. *ISME J.* **10**, 64–74 (2016).
6. Büttner, D. Behind the lines–actions of bacterial type III effector proteins in plant cells. *FEMS Microbiol. Rev.* **40**, 894–937 (2016).
7. Staehelin, C. & Krishnan, H. B. Nodulation outer proteins: double-edged swords of symbiotic rhizobia. *Biochem. J.* **470**, 263–274 (2015).
8. Camuel, A. et al. Widespread *Bradyrhizobium* distribution of diverse type III effectors that trigger legume nodulation in the absence of nod factor. *ISME J.* **17**, 1416–1429 (2023).
9. Ge, Y. Y. et al. The type 3 effector NopL of *Sinorhizobium* sp. strain NGR234 is a mitogen-activated protein kinase substrate. *J. Exp. Bot.* **67**, 2483–2494 (2016).
10. Neves, F. P. et al. The economic importance of the peanuts production chain. *Rev. Bras. Eng. Biossistemas* **17**, (2023).

11. Asante, M., Ahiabor, B. D. K. & Atakora, W. K. Growth, nodulation, and yield responses of groundnut (*Arachis hypogaea* L.) as influenced by combined application of Rhizobium inoculant and phosphorus in the Guinea Savanna Zone of Ghana. *Int. J. Agron.* 8691757 (2020).
12. Valetti, L. et al. Development and field evaluation of liquid inoculants with native bradyrhizobial strains for peanut production. *Afr. Crop Sci. J.* **24**, 1–13 (2016).
13. Palai, J., Malik, G., Maitra, S. & Banerjee, M. Role of *Rhizobium* on growth and development of groundnut: a review. *IJAEB*. **14**, 63–73 (2021).
14. Noisangiam, R. et al. Genetic diversity, symbiotic evolution, and proposed infection process of *Bradyrhizobium* strains isolated from root nodules of *Aeschynomene americana* L. in Thailand. *Appl. Environ. Microbiol.* **78**, 6236–6250 (2012).
15. Okazaki, S. et al. Genome analysis of a novel *Bradyrhizobium* sp. DOA9 carrying a symbiotic plasmid. *PLOS ONE*. **10**, e0117392 (2015).
16. Songwattana, P. et al. Type 3 secretion system (T3SS) of *Bradyrhizobium* sp. DOA9 and its roles in legume symbiosis and rice endophytic association. *Front. Microbiol.* **8**, (2017).
17. Piromyou, P. et al. *The new putative type III effector SkP48 in Bradyrhizobium sp. DOA9 is involved in legume nodulation*. https://www.researchsquare.com/article/rs-900464/v1 doi: (2021). https://doi.org/10.21203/rs.3.rs-900464/v1
18. Ratu, S. T. N. et al. Multiple domains in the rhizobial type III effector Bel2-5 determine symbiotic efficiency with soybean. *Front. Plant. Sci.* **12**, (2021).
19. Yadav, R., Chaudhary, S. & Ramakrishna, W. SUMO and SUMOylation in plants: ignored arsenal to combat abiotic stress. *Plant. Mol. Biol. Rep.* **42**, 34–47 (2024).
20. Wilkinson, K. A. & Henley, J. M. Mechanisms, regulation and consequences of protein SUMOylation. *Biochem. J.* **428**, 133–145 (2010).
21. Xiang, Q. W. et al. NopD of *Bradyrhizobium* sp. XS1150 possesses SUMO protease activity. *Front. Microbiol.* **11**, 386 (2020).
22. Riabroy, K. et al. Promising line KKBNM54-16-8, high yielding and peanut bud necrosis disease resistance. *KAJ*. **50**, 470–477 (2022).
23. de Bolzan, S., Deakin, W. J., Broughton, W. J. & Passaglia, L. M. P. Roles of flavonoids and the transcriptional regulator TtsI in the activation of the type III secretion system of *Bradyrhizobium elkanii* SEMIA587. *Microbiology* 157, 627–635 (2011).
24. Taurian, T. et al. Signal molecules in the peanut–bradyrhizobia interaction. *Arch. Microbiol.* **189**, 345–356 (2008).
25. Cesari, A. et al. Restrictive water condition modifies the root exudates composition during peanut-PGPR interaction and conditions early events, reversing the negative effects on plant growth. *Plant. Physiol. Biochem.* **142**, 519–527 (2019).
26. Guha, S. et al. Nod factor-independent 'crack-entry' symbiosis in dalbergoid legume *Arachis hypogaea*. *Environ. Microbiol.* **24**, 2732–2746 (2022).
27. Lai, Y. et al. Structure and function of type III secretion system in peanut *Bradyrhizobium* sp. MM6. *Acta Microbiol. Sin*. **60**, 476–485 (2020).
28. Shang, J. Y. et al. Coordinated regulation of symbiotic adaptation by NodD proteins and NolA in the type I peanut bradyrhizobial strain *Bradyrhizobium zhanjiangense* CCBAU51778. *Microbiol. Res.* **265**, 127188 (2022).
29. Faruque, O. M. et al. Identification of *Bradyrhizobium elkanii* genes involved in incompatibility with soybean plants carrying the *Rj4* allele. *Appl. Environ. Microbiol.* **81**, 6710–6717 (2015).
30. Li, Y. H. et al. *Bradyrhizobium nanningense* sp. nov., *Bradyrhizobium guangzhouense* sp. nov. and *Bradyrhizobium zhanjiangense* sp. nov., isolated from effective nodules of peanut in Southeast China. *Syst. Appl. Microbiol.* **42**, 126002 (2019).
31. Bosse, M. A. et al. Physiological impact of flavonoids on nodulation and ureide metabolism in legume plants. *Plant. Physiol. Biochem.* **166**, 512–521 (2021).
32. Hungria, M., Joseph, C. M. & Phillips, D. A. *Rhizobium nod* gene inducers exuded naturally from roots of common bean (*Phaseolus vulgaris* L.). *Plant Physiol.* 97, 759–764 (1991).
33. Yeh, K. C., Peck, M. C. & Long, S. R. Luteolin and GroESL modulate *in vitro* activity of NodD. *J. Bacteriol.* **184**, 525–530 (2002).
34. Li, F., Hou, B., Chen, L., Yao, Z. & Hong, G. Vitro *vitro* observation of the molecular interaction between NodD and its inducer naringenin as monitored by fluorescence resonance energy transfer. *Acta Biochim. Biophys. Sin*. **40**, 783–789 (2008).
35. Wang, J. et al. Transcriptomic and metabolomic analyses reveal the roles of flavonoids and auxin on peanut nodulation. *Int. J. Mol. Sci.* **24**, 10152 (2023).
36. Lee, W. K., Jeong, N., Indrasumunar, A., Gresshoff, P. M. & Jeong, S. C. *Glycine max* non-nodulation locus*rj1*: A recombinogenic region encompassing a SNP in a lysine motif receptor-like kinase (*GmNFR1α*). *Theor. Appl. Genet.* **122**, 875–884 (2011).
37. Diepold, A. & Wagner, S. Assembly of the bacterial type III secretion machinery. *FEMS Microbiol. Rev.* **38**, 802–822 (2014).
38. Liu, D. et al. TRAPPC13 is a novel target of *Mesorhizobium amorphae* type III secretion system effector NopP. *Mol. Plant-Microbe Interactions®*. **34**, 511–523 (2021).
39. Li, S. J. & Hochstrasser, M. A new protease required for cell-cycle progression in yeast. *Nature*. **398**, 246–251 (1999).
40. Nissan, G. et al. The type III effectors HsvG and HsvB of gall-forming *Pantoea agglomerans* determine host specificity and function as transcriptional activators. *Mol. Microbiol.* **61**, 1118–1131 (2006).
41. De Lange, O. et al. Breaking the DNA-binding code of *Ralstonia solanacearum* TAL effectors provides new possibilities to generate plant resistance genes against bacterial wilt disease. *New. Phytol.* **199**, 773–786 (2013).
42. Karmakar, K. et al. Transcriptomic analysis with the progress of symbiosis in 'crack-entry' legume *Arachis hypogaea* highlights its contrast with 'infection thread' adapted legumes. *Mol. Plant-Microbe Interactions®*. **32**, 271–285 (2019).
43. del Cerro, P. et al. Engineered CaM2 modulates nuclear calcium oscillation and enhances legume root nodule symbiosis. *Proc. Natl. Acad. Sci.* 119, e2200099119 (2022).
44. Lefebvre, B. et al. A remorin protein interacts with symbiotic receptors and regulates bacterial infection. *Proc. Natl. Acad. Sci.* **107**, 2343–2348 (2010).
45. Yano, K. et al. CERBERUS, a novel U-box protein containing WD-40 repeats, is required for formation of the infection thread and nodule development in the legume–*Rhizobium* symbiosis. *Plant. J.* **60**, 168–180 (2009).
46. Hervé, C., Lefebvre, B. & Cullimore, J. How many E3 ubiquitin ligase are involved in the regulation of nodulation? *Plant. Signal. Behav.* **6**, 660–664 (2011).
47. Tonelli, M. L., Figueredo, M. S., Rodríguez, J., Fabra, A. & Ibañez, F. Induced systemic resistance-like responses elicited by rhizobia. *Plant. Soil.* **448**, 1–14 (2020).
48. Du, M. et al. MYC2 orchestrates a hierarchical transcriptional cascade that regulates jasmonate-mediated plant immunity in tomato. *Plant. Cell.* **29**, 1883–1906 (2017).
49. Bertini, L. et al. Pathogen-responsive wheat *PR4* genes are induced by activators of systemic acquired resistance and wounding. *Plant. Sci.* **164**, 1067–1078 (2003).
50. Serrazina, S., Machado, H., Costa, R. L., Duque, P. & Malhó, R. Expression of *Castanea crenata* allene oxide synthase in arabidopsis improves the defense to *Phytophthora cinnamomi*. *Front. Plant. Sci.* **12**, 628697 (2021).
51. Piromyou, P. et al. The *Bradyrhizobium diazoefficiens* type III effector NopE modulates the regulation of plant hormones towards nodulation in *Vigna radiata*. *Sci. Rep.* **11**, 16604 (2021).
52. Vincent, J. M. A manual for the root-nodule bacteria. *Man. Root-Nodule Bact.* (1970).
53. Sadowsky, M. J., Tully, R. E., Cregan, P. B. & Keyser, H. H. Genetic diversity in *Bradyrhizobium japonicum* Serogroup 123 and its relation to genotype-specific nodulation of soybean. *Appl. Environ. Microbiol.* **53**, 2624–2630 (1987).
54. Sambrook, J., Fritsch, E. & Maniatis, T. *Molecular Cloning: A Laboratory Manual* 2nd edn (Cold Spring Harbor, 1989).
55. Tsai, J. W. & Alley, M. R. K. Proteolysis of the McpA chemoreceptor does not require the *Caulobacter* major chemotaxis operon. *J. Bacteriol.* **182**, 504–507 (2000).

56. Giraud, E., Lavergne, J. & Verméglio, A. Chapter 9 - Characterization of bacteriophytochromes from photosynthetic bacteria: Histidine kinase signaling triggered by light and redox sensing. in *Methods in Enzymology* vol. 471 135–159 (2010).
57. Wongdee, J., Boonkerd, N., Teaumroong, N., Tittabutr, P. & Giraud, E. Regulation of nitrogen fixation in *Bradyrhizobium* sp. strain DOA9 involves two distinct NifA regulatory proteins that are functionally redundant during symbiosis but not during free-living growth. *Front. Microbiol.* **9**, (2018).
58. Wongdee, J. et al. nifDK clusters located on the chromosome and megaplasmid of *Bradyrhizobium* sp. strain DOA9 contribute differently to nitrogenase activity during symbiosis and free-living growth. *Mol. Plant-Microbe Interactions®*. **29**, 767–773 (2016).
59. Ehrhardt, D. W., Atkinson, E. M. & Long, S. R. Depolarization of alfalfa root hair membrane potential by *Rhizobium meliloti* nod factors. *Science*. **256**, 998–1000 (1992).
60. Renier, A. et al. Photosynthetic *Bradyrhizobium* sp. strain ORS285 synthesizes 2-O-Methylfucosylated lipochitooligosaccharides for nod gene–dependent interaction with *Aeschynomene* plants. *Mol. Plant-Microbe Interactions®*. **24**, 1440–1447 (2011).
61. Wangthaisong, P. et al. The type IV secretion system (T4SS) mediates symbiosis between *Bradyrhizobium* sp. SUTN9-2 and legumes. *Appl. Environ. Microbiol.* **89**, e00040–e00023 (2023).
62. Babst, M., Hennecke, H. & Fischer, H. M. Two different mechanisms are involved in the heat-shock regulation of chaperonin gene expression in *Bradyrhizobium japonicum*. *Mol. Microbiol.* **19**, 827–839 (1996).
63. Livak, K. J. & Schmittgen, T. D. Analysis of relative gene expression data using real-time quantitative PCR and the 2− ΔΔCT method. *Methods*. **25**, 402–408 (2001).
64. Vallenet, D. et al. MicroScopean integrated microbial resource for the curation and comparative analysis of genomic and metabolic data. *Nucleic Acids Res.* **41**, D636–D647 (2013).
65. Nguyen, L. T., Schmidt, H. A., Von Haeseler, A. & Minh, B. Q. IQ-TREE: a fast and effective stochastic algorithm for estimating maximum-likelihood phylogenies. *Mol. Biol. Evol.* **32**, 268–274 (2015).
66. Kalyaanamoorthy, S., Minh, B. Q., Wong, T. K., Von Haeseler, A. & Jermiin, L. S. ModelFinder: fast model selection for accurate phylogenetic estimates. *Nat. Methods*. **14**, 587–589 (2017).
67. Hoang, D. T., Chernomor, O., Von Haeseler, A., Minh, B. Q. & Vinh, L. S. UFBoot2: improving the ultrafast bootstrap approximation. *Mol. Biol. Evol.* **35**, 518–522 (2018).

Acknowledgements

This work was supported by (i) Suranaree University of Technology (SUT), (ii) One Research One Graduate (OROG) of SUT Fund, (iii) Thailand Science Research and Innovation (TSRI), (iv) National Science, Research and Innovation Fund (NSRF), (v) JSPS-NRCT by National Research Council of Thailand (grant number N11A670769), (vi) the NSRF via the Program Management Unit for Human Resources & Institutional Development, Research and Innovation [grant number B16F640113] and (vii) French National Research Agency ("ET-Nod"; ANR-20-CE20-0012).

Author contributions

Author contributions Contributions B.A., P.P., P.B., P.S., J.W., T.G., K.T., P.T., N.B., E.G. and N.T. designed the experiments. B.A., P.S, P.P., P.B.,A.C., P.T. and E.G. performed the experiments and analysed the data. B.A., P.S., P.B., E.G. and N.T. wrote the paper.

Declarations

Competing interests

The authors declare no competing interests.

Additional information

Supplementary Information The online version contains supplementary material available at https://doi.org/10.1038/s41598-024-78913-2.

Correspondence and requests for materials should be addressed to E.G. or N.T.

Reprints and permissions information is available at www.nature.com/reprints.

Publisher's note Springer Nature remains neutral with regard to jurisdictional claims in published maps and institutional affiliations.

Open Access This article is licensed under a Creative Commons Attribution-NonCommercial-NoDerivatives 4.0 International License, which permits any non-commercial use, sharing, distribution and reproduction in any medium or format, as long as you give appropriate credit to the original author(s) and the source, provide a link to the Creative Commons licence, and indicate if you modified the licensed material. You do not have permission under this licence to share adapted material derived from this article or parts of it. The images or other third party material in this article are included in the article's Creative Commons licence, unless indicated otherwise in a credit line to the material. If material is not included in the article's Creative Commons licence and your intended use is not permitted by statutory regulation or exceeds the permitted use, you will need to obtain permission directly from the copyright holder. To view a copy of this licence, visit http://creativecommons.org/licenses/by-nc-nd/4.0/.

© The Author(s) 2024